Influence of film thickness and Ar—N_2 plasma gas on the structure and performance of sputtered vanadium nitride coatings

Linda Aissani[a,b], Akram Alhussein[c,*], Corinne Nouveau[d], Laala Ghelani[e], Mourad Zaabat[b]

[a] *Physics Department, ABBES Laghrour- Khenchela University, P.O. 1252, 40004, Algeria*
[b] *Laboratory of Active Components and Materials, Larbi Ben M'Hidi University, Oum El Bouaghi 04000, Algeria*
[c] *ICD–LASMIS, Université de Technologie de Troyes, CNRS, Antenne de Nogent, Pôle Technologique Sud Champagne, 26 Rue Lavoisier, 52800 Nogent, France*
[d] *Arts et Métiers ParisTech, La.Bo.Ma.P, Rue Porte de Paris, 71250 Cluny, France*
[e] *Mechanical Engineering Department, ABBES Laghrour- Khenchela University, P.O. 1252, 40004, Algeria*

ARTICLE INFO

Keywords:
V—N films
Magnetron sputtering
Microstructure
Mechanical properties
Tribological properties

ABSTRACT

We investigated the effect of film thickness on the structure and properties of V—N coatings deposited by magnetron sputtering in an argon and nitrogen atmosphere. The nitrogen percentage was changed between 10 and 20%. Firstly, structural and morphological properties of V—N films were observed, analyzed and subsequently followed by a detailed investigation on the mechanical and tribological properties of these coatings.

It has been shown that film structure, hardness and wear resistance significantly changed with varying the film thickness and the nitrogen percentage. In the case of films deposited under 10%N_2, the presence of V_2N phase was evident. With increasing nitrogen ratio in the deposition chamber from 10 to 20%, the structure was changed from (hc)V_2N to multi phases of V_2N and (fcc) VN (formation of different vanadium nitrides). The thick films containing more nitrogen were slightly dense compared to the thinner ones presenting rough surface and columnar morphology.

Nanoindentation measurements showed that film mechanical behavior depends on its thickness, nitrogen percentage and microstructural features. The film hardness first increased with its thickness and then decreased. The highest hardness of 26.2 GPa was obtained for the film deposited under 20%N_2, which is correlated with its dense structure and film stoichiometry.

The film thickness has a significant effect on the tribological properties of V—N films. The minimum friction coefficient of 0.4 was found for the thickest film of 2500 nm. The wear rate gradually decreased with increasing the film thickness, due to the high hardness, presence of VN phase and the strong adhesion between film and substrate.

1. Introduction

The improvement of surface hardness and wear resistance of parts made of steel would significantly increase the use of these materials. One of the possibilities of enhancing the mechanical properties of steel is to deposit hard coatings with CVD and PVD techniques [1]. The nitrogen with metals has very promising physical characteristics due to its high chemical and physical stability. The good properties of metallic nitrides allow to be used in many applications under several service conditions [2].

Among the sputtered nitride films, vanadium nitrides offer excellent properties and present high corrosive resistance against aggressive media, and good oxidation resistance in ambient air at high temperature [3–6]. In addition, the V—N films were known to show a decrease in the friction coefficient with an increase in temperature due to the formation and melting of V_2O_5 on the wear track during friction process [6,7]. This condition is favorable for cutting tools under high speed machining without lubrication that makes it a suitable compound for many uses [8–10].

The mechanical properties of the films are essentially influenced by the crystallographic structure, which is established during the film deposition. V—N films with an almost stoichiometric composition exhibit cubic or hexagonal structures and hence present higher hardness values than the other nitrides films [11–14].

Depending on the deposition conditions, the sputtered V—N coatings could be deposited with nanometric particles, displaying very high hardness values (up to 30 GPa) and a low coefficient of friction (0.4) compared to any other binary compounds [15,16].

* Corresponding author.
E-mail address: akram.alhussein@utt.fr (A. Alhussein).

The V−N films are very sensitive to the variation of the deposition parameters [7,10]. Our goal is to obtain films with a pure phase, free strain and fine particles with controlled morphology. Interestingly, Krause et al. have reported the microstructure–property relationship of reactive magnetron sputtered V−N films deposited at different deposition angles [17]. In our recent study, we evaluated the influence of nitrogen partial pressure on the microstructure and mechanical and tribological behavior of V-C-N coatings [18]. Qiu et al. have investigated the effect of nitrogen pressure and negative substrate bias on the microstructure and the mechanical performance of V−N films [19]. Guo et al. have reported the effect of deposition temperature on the microstructure, mechanical and tribological properties of V−N films deposited by Pulsed Laser Deposition technique (PLD) [20].

Compared to TiN and CrN, we can find few research examples focused on the effects of both film thickness and nitrogen percentage on crystalline phases or preferred orientation of the sputtered V−N coatings [7]. Furthermore, the changes in hardness, Young's modulus and friction coefficient of V−N films deposited on steel have not yet been thoroughly studied.

The crystal structure and texture of the grown V−N films are dependent on the ratio of N_2/Ar in the reactive gas mixture during deposition [7,21]. The optimal composition of the V−N sputtered coatings was selected to explore the phase formation mechanism and its properties. The structure of V−N films significantly transforms from (hc) V_2N to (fcc) VN phase with the increase of nitrogen content.

The ability for VN solid solution structure formation depends on the nitrogen insertion between the vanadium atoms; which can help to provide new insights to understand the phase formation mechanism of vanadium nitride thin film with different nitrogen content. In addition, it has been reported that the texturing is strongly influenced by film thickness. Furthermore, V−N compounds were found to be thermodynamically stable, with a wide range of stoichiometry 0.5 to 1. Therefore, simultaneous determination of composition and crystal structure becomes important in order to obtain stoichiometric films with best mechanical properties [22,23].

For this reason, the fundamental analysis of the influence of the deposition parameters on the structure as well as mechanical and tribological properties is required, in order to suitably adjust the properties of V−N films. In this paper, we present the influence of varying of film thickness and nitrogen percentage in the deposition gas atmosphere on V−N coatings' crystal structure, elemental composition, microstructure evolution, morphology and eventually mechanical and tribological behavior with an advantage of being able to produce excellent mechanical and physicochemical properties.

2. Experimental setup

The V−N films were deposited on Si (100) (1 × 1 cm^2, 450 μm) and XC100 steel substrates (Ø 15 × 3 mm) by the magnetron sputtering technique (NORDIKO type 3500, 13.56 MHz). V−N films were obtained by sputtering of vanadium target (99.9% purity, 10.6 cm of diameter and 3 mm thick) in an argon and nitrogen atmosphere. The nitrogen to argon ratios were: N_2/Ar = 11.1 and 25% corresponding to gas flow rates of 10:90 sccm and 20:80 sccm, respectively. These both configurations led to obtain binary films with N/V ratios equal to 0.5 and 1, respectively.

The samples were placed on a substrate-holder in front of the V target at 80 mm. Before deposition, the chamber was evacuated to a low pressure of 2×10^{-5} Pa. The samples were cleaned in ultrasonic bath by acetone and ethanol (5 min for each one) and dried in air. Prior to deposition, the vanadium target and substrates were cleaned by Ar^+ ions bombardment for 5 min at 0.4 Pa, applying a voltage (applied power) of −700 V (350 W) and −500 V (250 W), respectively. The deposition of films was carried out, without rotating the sample-holder, at constant working pressure and temperature of 0.4 Pa and 150 °C, respectively. The deposition duration was varied between 20 and 180 min to obtain films with different thicknesses in the range of 260–2500 nm.

The crystallographic structures of V−N films were analyzed by X-Ray Diffraction (XRD) using a Bruker D8 Advance diffractometer with Co cathode (Co–Kα radiation λ = 1.78 Å). A θ-2θ scan was performed for 2θ diffraction angles ranging from 20° to 80° with a scan step of 0.01° recorded during 2 s.

The binding energy and chemical composition of the V−N films were determined by X-Ray Photoelectron Spectroscopy (XPS). The experiments were performed in a Riber SIA 100 spectrometer with a non-monochromatic X-ray source ($Al_{K\alpha}$ line of 1486.6 eV energy), an applied power of 300 W and a vacuum pressure of 4×10^{-8} Pa. The calibration was done using the line of C1s at 284.8 eV with a full width at half maximum (FWHM) of 1.1 eV, which was absorbed on the surface of the samples. Prior XPS analysis, the (Ar^+) ion bombardment with 3 keV of primary energy was sputtered on the sample for 3 min to clean all coating surfaces and to increase the reliability of chemical analysis [10]. The corresponding V2p, N1s and O1s spectra were fitted under a multi-peak fitting method, and the ratio of Lorentzian to Gaussian was 20% [12]. Casa XPS software tool was used for XPS peak fitting for this analysis.

For supplementary identification of the as-deposited films phases, Raman spectroscopy with a Bruker Senterra spectrometer was applied. Exciting laser radiation wavelength was 600 nm. This identification was supported by a reference Raman spectrum of phases expected in V−N coatings.

The surface morphology and cross section of the coatings were observed using a Scanning Electron Microscope (SEM-Joel JSM-6400F, 10 kV). The SEM was equipped with EDS microanalysis (Oxford INCA x-act, 15 kV) used for chemical composition analysis. The concentration of V and N quantified by this technique was compared with the XPS data.

The film surface roughness was measured by an Atomic Force Microscope (AFM 100, APE research), which was employed under contact mode with a scanning range of 3 × 3 μm^2. The AFM tests were carried out using a V-shaped high resonance frequency silicon nitride cantilever with a pyramidal tip of 50 nm radius and applying a constant force of 0.032 N/m.

The mechanical properties (hardness and Young's modulus) of V−N films were measured by using a Nanoindenter XP (MTS-XP) system in continuous stiffness mode having a diamond indenter (Berkovich tip), with a tip radius of 200 nm. The mechanical properties were calculated using the Oliver-Pharr method [23]. The hardness values were determined from the average of five indentations and were evaluated at a depth of 10% of the total film thickness in order to avoid the influence of substrate and surface roughness.

The residual stresses of the V−N films deposited on the Si (100) wafers were determined by an interferometer (Newton's rings method [3,22]) and calculated with the following Stoney's formula [24]:

$$\sigma = \frac{Es}{6(1-\nu_s)}\frac{t_s^2}{t_f}\left(\frac{1}{R}-\frac{1}{R_0}\right) \quad (1)$$

where E_s (181 GPa) and ν_s (0.28) are Young's modulus and Poisson's ratio of Si (100), respectively. t_s and t_f are the thickness of the Si (100) wafer and the deposited film, respectively, while R_0 and R are the curvature radius before and after deposition, respectively [25].

The tribological characterization was carried out by means of sliding wear tests, using a tribometer (TRIBO tester) under a ball-on-disc configuration. For this purpose, a 6 mm diameter 100Cr6 ball was used as counterpart, with an applied normal load of 2 N, a sliding distance of 200 m and a constant speed of 5 cm s^{-1}. The depth and wear rates were determined by means of an optical 3D profilometer (VEECO, Wyko-NT 1100) [6]. The worn wear tracks were observed and measured by means of a SEM.

Table 1
Film thickness, surface roughness and chemical composition (at.%) of V−N coatings.

Deposition time (min)	Thickness (nm)	Ra(nm)	V		N		O		N/V	
			EDS	XPS	EDS	XPS	EDS	XPS	EDS	XPS
20%N_2										
20	260	54.0	48.4	48.0	46.0	46.5	5.6	5.5	0.95	0.97
30	300	50.5	47.7	47.0	45.7	46.0	6.6	7.0	0.96	0.98
60	600	47.0	50.1	49.0	47.3	48.0	2.6	3.0	0.94	0.98
90	960	28.2	47.8	47.0	48.8	49.0	3.4	4.0	1.02	1.04
120	1500	11.6	48.2	48.5	49.5	50.0	2.3	1.5	1.03	1.03
180	1800	8.5	47.0	47.5	50.1	50.0	2.9	2.5	1.07	1.05
10%N_2										
20	300	42.0	65.0	65.0	29.1	29.0	5.9	6.0	0.45	0.44
30	400	55.9	64.3	65.0	31.3	31.0	4.4	4.0	0.49	0.48
60	950	68.5	64.6	65.0	32.5	32.0	2.9	3.0	0.50	0.49
90	1200	65.7	66.3	66.5	32.0	32.0	1.7	1.5	0.48	0.48
120	1800	75.6	64.6	65.0	33.5	33.5	1.9	1.5	0.52	0.51
180	2500	74.5	65.3	66.0	32.8	33.0	1.9	1.0	0.50	0.50

3. Results and discussion

3.1. Chemical composition

The chemical composition (determined by EDS and XPS analysis) and film thickness (determined by SEM) of V−N coatings, deposited under two different mixture atmospheres (N_2/Ar = 11.1 and 25%) are shown in Table 1. As the nitrogen percentage increased from 10 to 20%, the V content decreased from (65–64.3) to (47–50.1) at. %. This is mainly due to the uptake of nitrogen by the deposited metal with the increase of the concentration of reactive nitrogen gas compared with argon and the target pollution [6,26]. We noticed that the V−N coatings have a significant oxygen content (Table 1). This is due to the low densification of these films favoring the incorporation of oxygen. The low densification and the rough surface of the thin films conduct to the apparition of more defaults in the films and favorite the insertion of oxygen during film deposition. In addition, the mixing of these vanadium and nitrogen, during deposition, can form a strong base for the formation of oxides. The oxygen contamination may be due to the residual oxygen in the deposition chamber, the leak during coating deposition [6] or the chemical reaction of samples with air.

According to the EDS and XPS analysis, we observed the existence of nitrogen stoichiometry (N/V ≈ 1) in the case of V−N coatings deposited under 20%N_2. However, at 10%N_2, the N/V ≈ 0.5 confirms that film composition does not depend on its thickness. Addition of nitrogen led to significantly reduce the vanadium concentration and the film thickness. During the deposition, the total pressure of Ar−N_2 mixture gas was kept constant at 0.4 Pa. Thus, the density of argon decreased gradually with the increase of N_2 rate and resulted in a lower efficiency of argon-ion bombardment of the vanadium target. In addition to the effect of low Ar gas density, the contamination of the target surface with formation of oxides was also an important factor. This was mainly due to the target poisoning, which resulted in a low sputtering yield [24].

3.2. V−N films morphology

Fig. 1 presents the SEM cross-sectional and surface morphology of the V−N films deposited in different N_2/Ar mixture atmospheres (10 and 20%N_2) for different deposition times (different thicknesses). The films thicknesses were measured from the SEM images and these values are presented in Table 1. From Fig. 1, it is obvious that increasing the deposition time of V−N films deposited under 20%N_2 led to change the film microstructure from columnar to dense one. The columnar growth is observed on the cross-sectional SEM images with a rough and coarse irregular surface surrounded by large grains for the thin film of small thickness (260 nm) (Fig. 1a). The morphology of the thicker films (960 and 1800 nm) exhibited a relatively smoother homogeneous surface with fine grains confirmed by a clear decrease in the roughness from 54 to 28.2 and 8.5 nm, respectively (Fig. 1b and c and Table 1). According to Mahieu's zone model, the structure of V−N films is attributed to the Ic zone, which is characterized by a dense and columnar structure [27]. This zone is characterized generally by polycrystalline faceted columns without preferential orientation [28].

The other V−N films deposited under 10%N_2 present columnar morphology. The V−N film of 1200 nm thick (Fig. 1e) has a porous and rough surface as compared to the thin film of 300 nm (Fig. 1d). The film surface roughness increases with its thickness (Fig. 1e and f). Increasing the film thickness led to increase the surface roughness from 42 nm to 75 nm (Table 1). This predicts the changes in the film structure as a function of the deposition duration. According to the Mahieu's structure zone model [27], this morphology is a mixture of both I and II zones characterized by a columnar structure separated by voids and V-shaped and faceted columns.

3.3. Microstructure analysis

Figs. 2 and 3 present the XRD patterns of V−N coatings deposited under 10 and 20%N_2 for different film thicknesses. At 10%N_2, for all coatings, the four diffraction peaks at 50°, 58°, 63.8° and 75.2° correspond to (111), (201), (112) and (110) crystalline planes of hexagonal V_2N phase (JCPDS card, No. 00-032-1413), respectively (Fig. 2). Meanwhile, the V−N coatings revealed minor diffraction peaks of (200) VN at 51.23° (JCPDS card, No.00-073-0528) and (110) V_2O_5 (JCPDS card, No. 18-1450) crystalline plane at 46°. At 20%N_2, the V−N coating exhibited (111), (200) and (220) diffraction planes at 42.3°, 50.6° and 71.2° corresponding to the face-centered cubic VN phase (JCPDS card, No.00-073-0528) (Fig. 3). We note the presence of the (112) V_2N crystalline plane at 64.5° in all films that confirms clearly the mixed phases of VN and V_2N formed in the coating. The peak positions of V−N films are at higher diffraction angles than that of VN and V_2N as compared with JCPDS data. This may suggest that V−N coatings consist of solid solution formed from VN and V_2N. The peaks shift is related to the oxygen contamination and the compressive residual stress (Table 2) generated by the ion bombardment at high applied power (650 W) [6]. It clearly shows that the major peak was changed from a (200) VN to a (111) VN with an increase in the nitrogen flow rate injected in the deposition chamber (from 10 to 20%N_2). The films deposited under 10%N_2 had a dual phase in which (200) VN is the major peak as compared with the weak (111) V_2N peak, influencing the film texture [29,30]. However, the (111) VN peak was shown clearly in the films deposited under 20%N_2. The VN phase confirmed by the EDS analysis

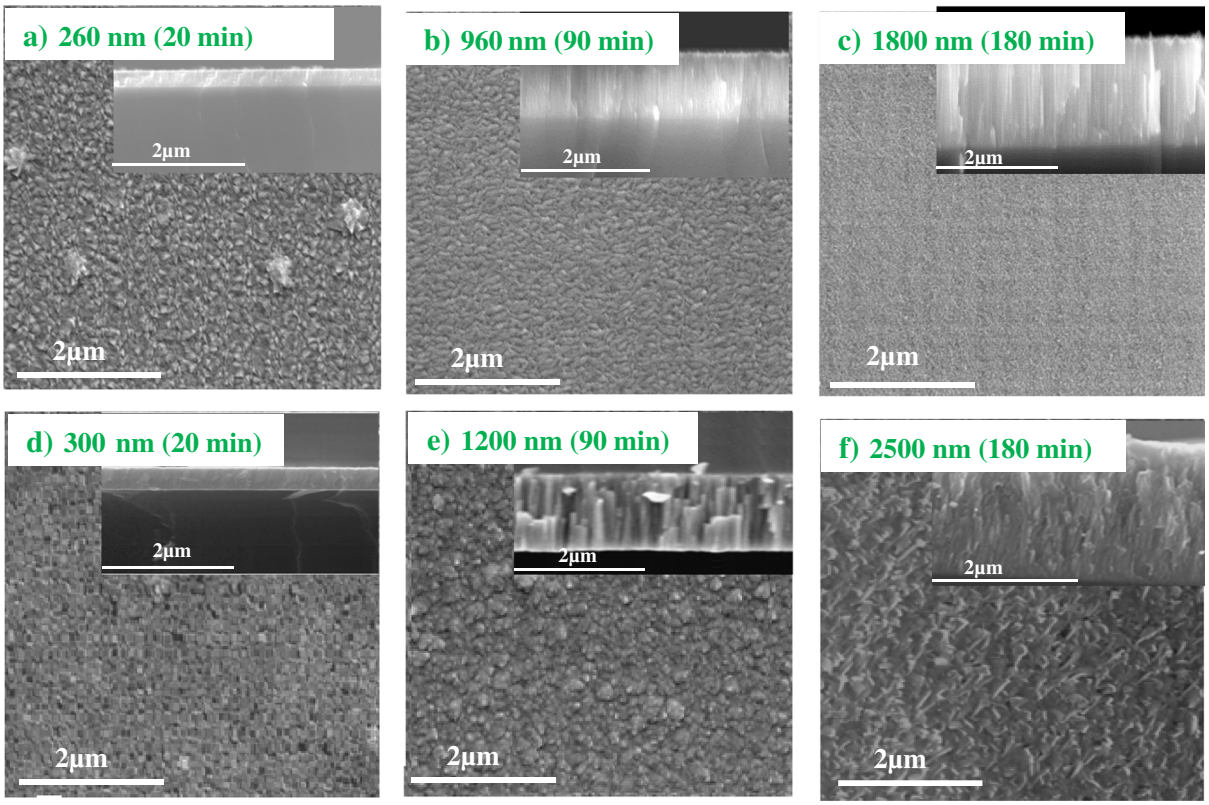

Fig. 1. SEM images of surface and cross-sections of V–N coatings sputtered under 20%N_2 for: a) 20, b) 90 and c) 180 min and under 10%N_2 for: d) 20, e) 90 and f) 180 min. Standard deviation of the thickness was about 10 nm.

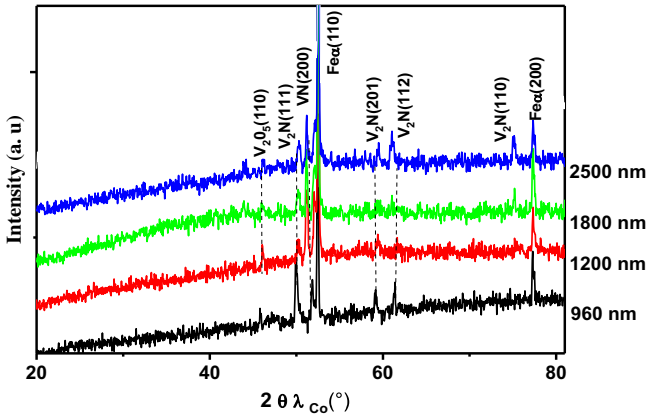

Fig. 2. XRD patterns of V–N coatings deposited under 10%N_2 for different film thicknesses.

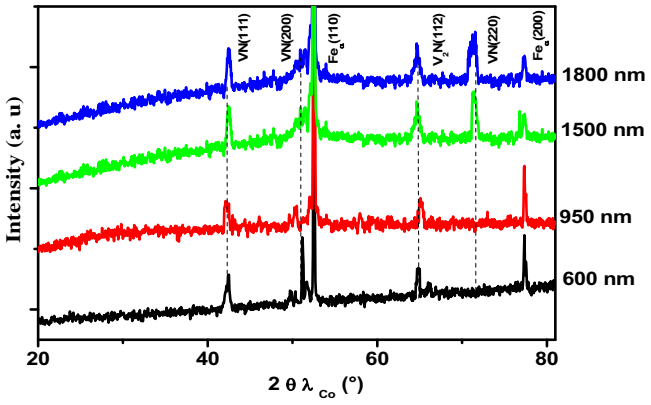

Fig. 3. XRD patterns of V–N coatings deposited under 20% N_2 for different film thicknesses.

indicates that the film was crystallized and consistent with the results given in Ref. [29]. The crystallite growth was strongly dependent on the thickness, and hence, the texture variation between the films. The texture dominant in thinner films is due to the high surface energy of (200) VN. The V–N thick films are textured along (111) planes presenting higher potential energy. The changes in preferred orientations and packing density with increasing the film thickness were observed in sputtered Ti–N films [3]. The dual phase of the V–N films deposited under 10% N_2 having a major (200) VN peak in parallel with the (111) V_2N peak can be explained by the higher ion bombardment which leads to the higher mobility of adatoms on the V–N film surface. The adatoms are more condensed but less arranged than those deposited at 20% N_2, which may result in lower film density.

As vanadium nitrides and oxides have different vibration modes [31], Raman spectrometry is a good complementary method to determine the film structure. Fig. 4 shows Raman spectra of V–N coatings deposited under 10 and 20%N_2 for 120 min previously characterized by XRD (Figs. 2 and 3). For all V–N coatings, Raman spectra

Table 2
Mechanical properties of V–N coatings.

20%N_2			10%N_2	
Deposition time (min)	σ (−GPa)	H^3/E^2(GPa)	σ (−GPa)	H^3/E^2(GPa)
20	2.06 ± 0.02	0.226	1.81 ± 0.02	0.204
30	2.00 ± 0.02	0.204	1.50 ± 0.02	0.150
60	1.50 ± 0.02	0.163	1.00 ± 0.02	0.134
90	1.05 ± 0.02	0.134	0.70 ± 0.02	0.097
120	0.91 ± 0.02	0.123	0.70 ± 0.02	0.077
180	0.80 ± 0.02	0.121	0.54 ± 0.02	0.073

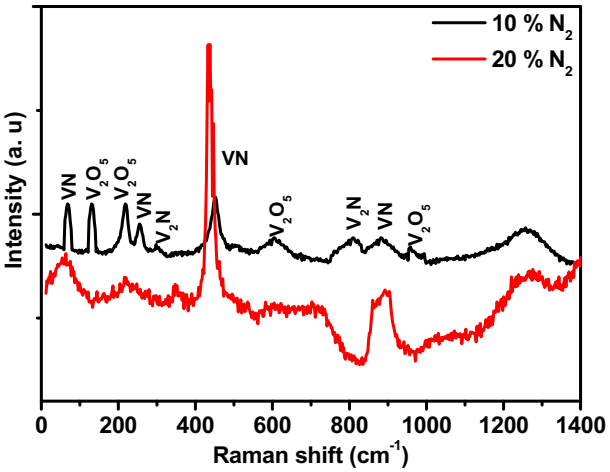

Fig. 4. Raman spectra of V−N coatings.

were similar. However, the V−N films deposited at 20% N_2 present a high intensity due to the high nitrogen percentage. The peaks located at 130, 230, 420, 890 and 910 cm^{-1} can be attributed to the typical modes of vanadium nitrides VN and V_2N [31–33]. This result is in agreement with that obtained from XRD. Hence, this demonstrates the formation of VN and V_2N bi-phases microstructure.

However, the data in literature concerning the V−N vibration modes are scarce. This is probably due to the low intensity of the scattered V−N peaks and to the presence of surface oxides on V−N coatings that display a very well resolved signature dominating the spectrum even if the oxides are present in low amounts (not detectable by XRD) [32]. As shown in Fig. 4, the V_2O_5 Raman bands were observed at both excitation wavelengths of 180, 270, 608 and 992 cm^{-1} that confirm the presence of vanadium oxide [31]. The formation of oxides in the V−N films was detected by Raman spectrometry and not by XRD for the film deposited under 20%N_2. Indeed, thermodynamically, the formation enthalpy of vanadium oxides, including V_2O_5 (-1491–1550 kJ mol^{-1}), is much higher than that of VN phase (-217 kJ mol^{-1}) [34].

In order to understand the chemical bonding states, the V−N coatings deposited under 20%N_2 were investigated by using XPS. The C1s peak at 284.6 eV was used as a reference to calibrate the XPS spectra. As seen in Fig. 5a, three contributions were found at 512.85, 513.93 and 515.18 eV ascribed to V−N and V−O, respectively [31]. The spectra of the films deposited, under 20%N_2, during 120 min (1500 nm) and 180 min (1800 nm) present a peak with a binding energy of 396.9 eV. This peak shown on the N1 s spectra is characteristic to VN (Fig. 5b) and gives a supplementary evidence supporting N element bonded to V during the coating deposition [6]. However, regarding the spectra of the film deposited for 120 min (900 nm), the N1 s was shifted to a higher binding energy (397.2 eV) compared to the VN reference [35]. The components observed would be related to the V_2N by the formation of V−N bonds. Furthermore, the formation of V−O bonds is corresponding to some trace of V_5O_9 formed by insertion of oxygen [6,36].

Fig. 6 presents the evolution of XPS spectra, taken in the V2p (a), N1 s (b) and O1s (c) core-level regions, for the films deposited under 10%N_2 as a function of their thickness. We obtained results very close to those of the coatings deposited at 20%N_2. The energy positions of the N1 s and O1s elements were 397.51 and 531.13 eV, respectively.

The V2p doublet shows a significant asymmetry with a higher binding energy side for the thick film (2500 nm) and requires at least three contributions. The major component has a binding energy of 514.01 eV, which is compatible with the V_2N [5,6,35,and]. The other minor peaks have binding energies of 513.81 and 515.70 eV corresponding to VN and V_2O_5, respectively. This can be attributed to the intermediate V oxides in the deposited films [36]. On the other hand, the V2p and N1 s peak intensities gradually increased while the FWHM decreased with increasing the film thickness. These results are in good agreement with those reported in the literature [36,37].

In order to analyze the V−N films phases, the lattice parameter and crystallite size were calculated from the V_2N and VN peaks. The shift of the peaks to higher diffraction angles reflects the decrease of the lattice parameter of V−N films from 4.160 ± 0.001 Å to 4.150 ± 0.001 Å (10% N_2) and from 4.176 ± 0.001 Å to 4.156 ± 0.001 Å (20% N_2) with increasing the film thickness (Fig. 7). However, the crystallite size gradually increased with decreasing the lattice parameter for all V−N coatings (Fig. 7). This behavior can be explained by the increase in the provided energy associated to the atoms bombarding the substrate surface during the film deposition. This induces an increase in the mobility of the pulverized vanadium atoms and reduces the number of defects in the crystallized areas, thus leads to decrease the lattice parameter. According to Huang et al., the decrease of lattice parameter and the increase of grain size can be explained by the increase of ion bombardment energy, the high residual stress and the incorporation of nitrogen atoms into the metal system [38].

3.4. Mechanical properties

Table 2 presents the mechanical properties (residual stress and H^3/E^2) of V−N coatings as a function of deposition N_2/Ar mixture atmosphere and film thickness. The evolutions of hardness (H) and Young's modulus (E) as a function of the film thickness for all the V−N films are shown in Fig. 8. From Table 2, it can be clearly seen that the compressive residual stress, generated in the V−N coatings during the deposition process, increased with the nitrogen percentage. This would be mainly due to the presence of compliant nitrogen with the structure of the V−N coatings. On the other hand, as the film thickness was gradually increased, a decreasing in the compressive residual stress was noticed: from -1.81 GPa (300 nm) to -0.54 GPa (2500 nm) for the films deposited under 10%N_2 and from -2.06 GPa (260 nm) to -0.80 GPa (1800 nm) for the films deposited under 20%N_2. As the columnar microstructure became dense at higher film thickness, the residual stress induced by sputtering could be released and consequently decreased. Meanwhile, the decrease in the compressive residual stress could be associated to the absence of a significant number of defects produced during the film growth [5].

The hardness is strongly related to the ionic binging energy of V−N and V−O formed in the crystals, the microstructure and the presence of porosity [39]. Earlier studies reported that (111) crystalline plane is the hardest one in the Ti−N film due to the geometrical strengthening [40]. Similar behaviour is expected for the V−N film having the same structure.

From Fig. 8, one can notice that films deposited for a short period of 20 and 30 min present high H and E values: 24 ± 0.4–22.5 ± 0.6 GPa and 279 ± 11–255 ± 11 GPa (for the films deposited under 10%N_2), and 26.2 ± 0.6–24 ± 0.6 GPa and 268 ± 11–255 ± 11 GPa (for the films deposited under 20%N_2), respectively. Increasing the film thickness led to decrease its hardness and Young's modulus. The lowest hardness and Young's modulus were obtained for the thickest film deposited for 180 min (Fig. 8). These values significantly remain higher than those of XC100 steel substrate (H = 6 ± 0.4GPa, E = 189 ± 11GPa) [6]. Comparing the hardness values of the two films deposited for 20 and 90 min under 10 and 20% of nitrogen shows that hardness decreased from 24 GPa to 15.3 GPa and from 26.2 GPa to 15.6 GPa, respectively. This is due to the decreased compressive stress and the densified structure. However, the hardness values of V−N films are lower than those reported by Kumar et al. [3].

With varying film thickness, the evolution of V−N films hardness is directly related to the microstructure, grain size and roughness [3,5]. The lowest hardness found at the highest penetration depth is due to the combination of film and substrate stiffness. Thus, the plastic deformation around the indentation zone was found on the interface between

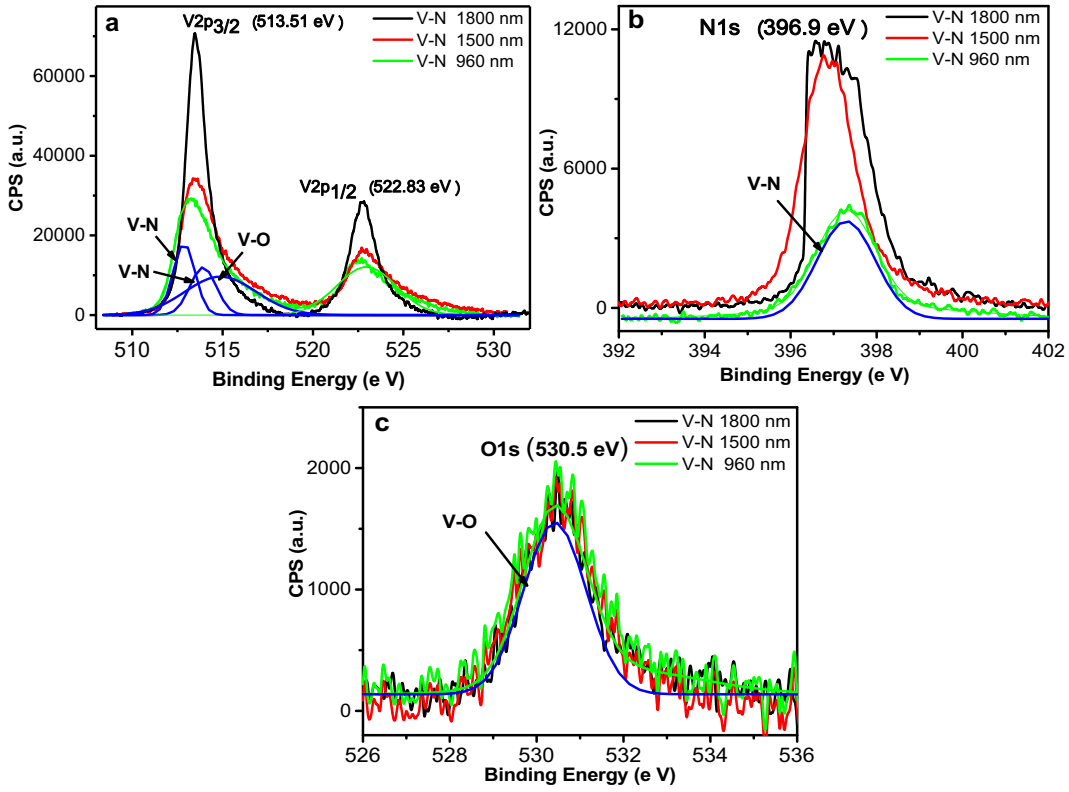

Fig. 5. Set of V2p (a), N1s (b) and O1s (c) core level spectra of V–N coatings deposited at 20%N_2 as a function of the film thickness.

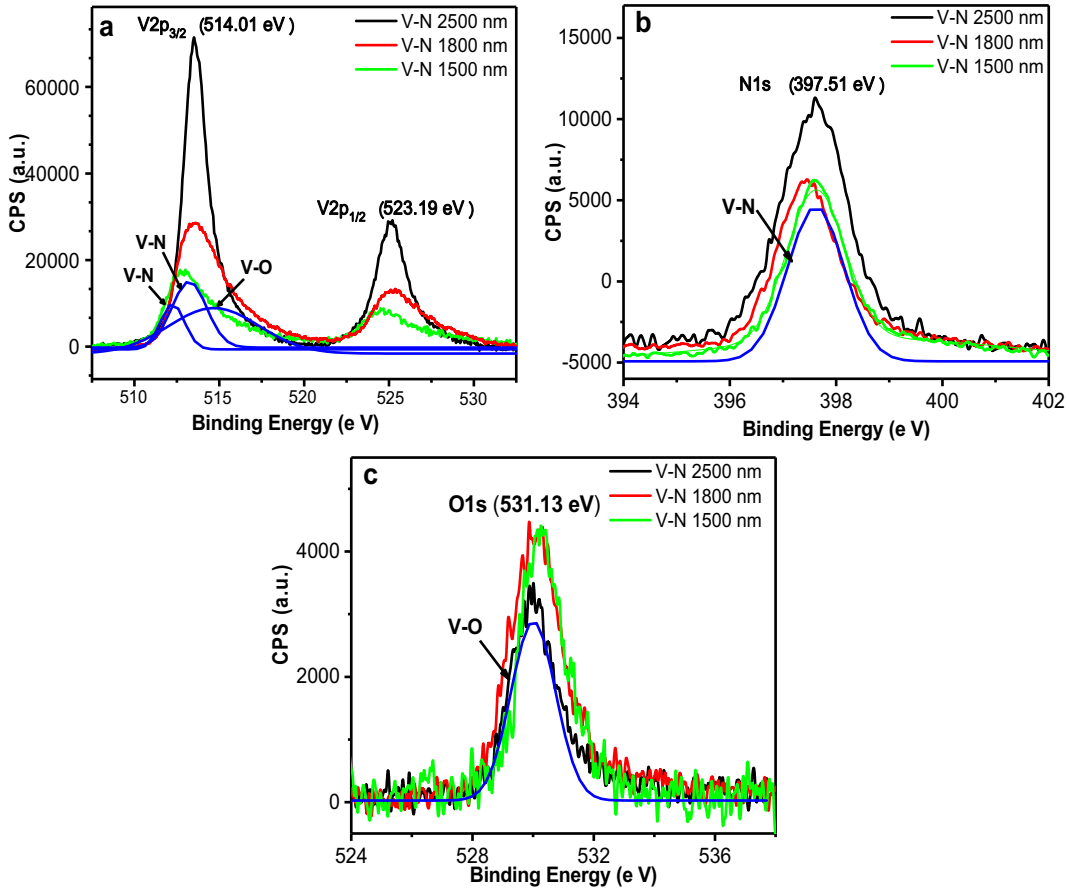

Fig. 6. Set of V2p (a), N1s (b) and O1s (c) core level spectra of V–N coatings deposited at 10%N_2 as a function of the film thickness.

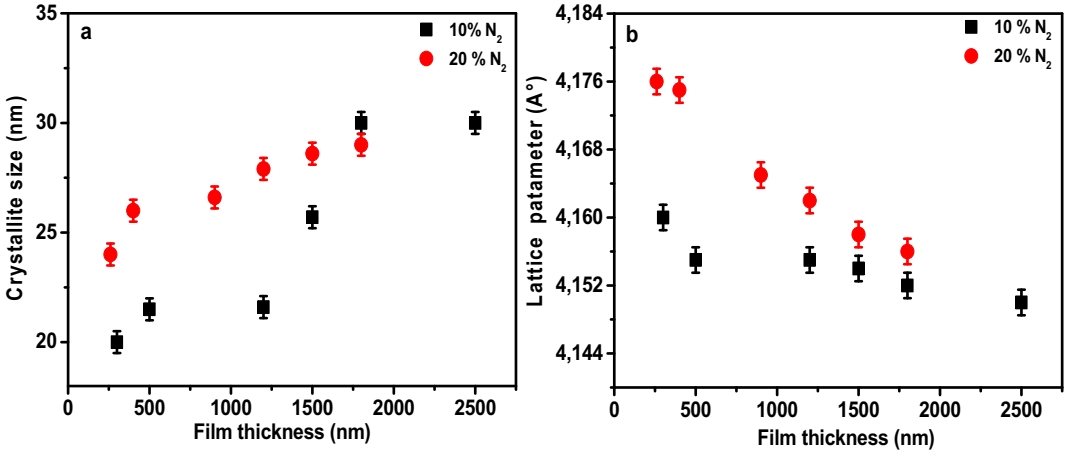

Fig. 7. Evolution of crystallite size (a) and lattice parameter (b) of V–N coatings as a function of the film thickness.

film and substrate. Moreover, porous, coarse surface and high residual stress might induce the propagation of cracks in the film/substrate interface because of the indentation size effect [3]. In these V–N films, the resistance against plastic deformation, which gives the relationship between hardness and Young's modulus (H^3/E^2), was high and decreased gradually with increasing the film thickness. Its value was between 0.204 and 0.073 GPa (for the films deposited under 10%N_2) and between 0.226 and 0.121 GPa (for the films deposited under 20%N_2), respectively (Table 2). It has been reported that the grain boundary sliding is the governing factor for dislocation motions in the film/substrate interface; and thus, it would decrease the mechanical properties [33]. With increasing the film thickness, the hardness and Young's modulus values stabilized at higher penetration depth for the films deposited under 10 and 20% N_2 and the plastic deformation zone did not reach nor affect the interface. This is directly related to the dense structure, the smooth surface and the low residual stress [3,6]. Furthermore, with increasing the nitrogen percentage up to 20% in the gas mixture atmosphere, a little increase in the hardness and Young's modulus values was observed. This is due to the refinement of the crystallite size, based on Hall–Petch effect [6], leading to a low surface roughness. In our work, the high hardness values for V–N films may be due to their high compressive stress and grain refinement [3,5]. In contrary, the coatings grown under 10%N_2 presented high roughness with large grains and high porosity, which explained the decrease in the resistance to the plastic deformation (H^3/E^2 ratio).

3.5. Tribological behaviour

3.5.1. Frictional behavior

Fig. 9 shows the variation of friction coefficient as a function of the

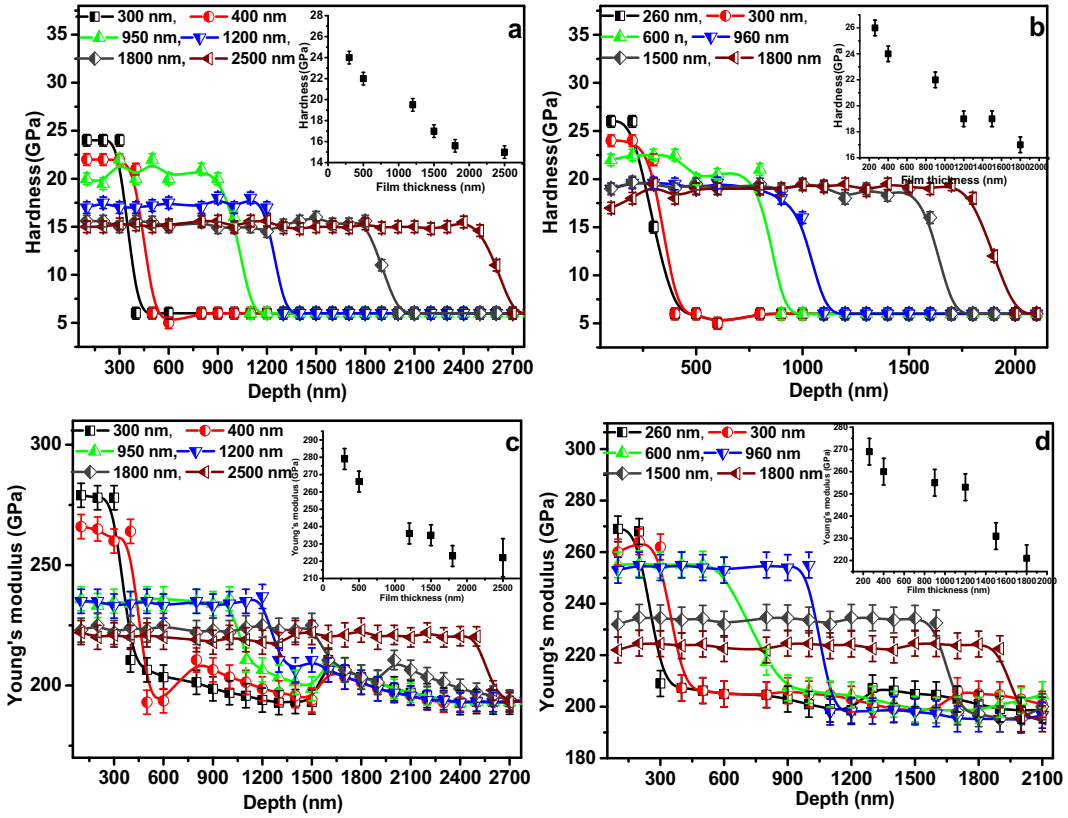

Fig. 8. Evolution of hardness and Young's modulus of V–N coatings deposited at (a, c) 10%N_2 and (b, d) 20%N_2 as a function of the film thickness.

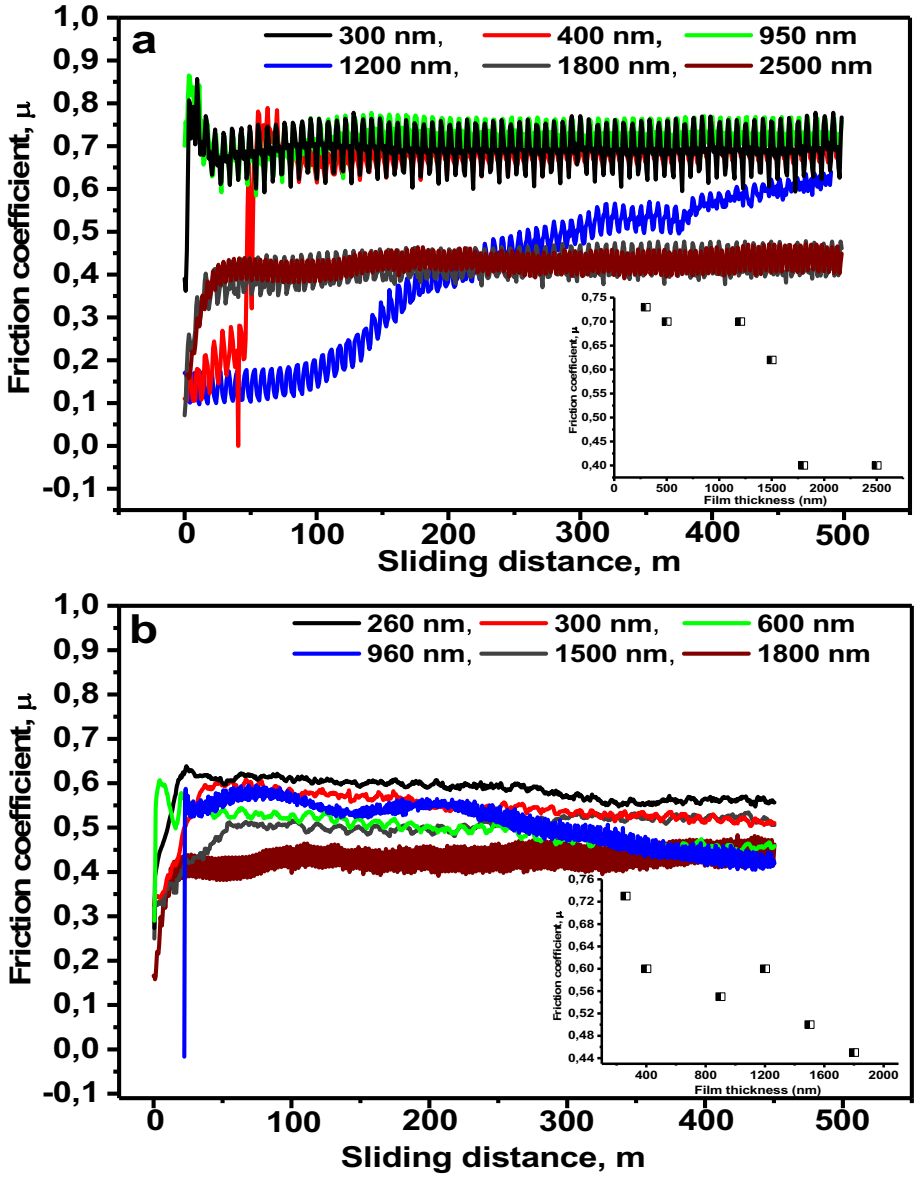

Fig. 9. Friction coefficient of V−N films deposited at: a) 10%N_2 and b) 20%N_2 for different film thicknesses.

sliding distance for the V−N films deposited under 10 and 20%N_2 (films with different thicknesses). The friction tests were carried out using a ball-on disc tribometer under dry sliding conditions. The friction coefficient values were determined from the stabilization zone where the curves seem quasi constant with increasing the sliding distance. The V−N films deposited for 20 min under 10 and 20%N_2 having respectively 300 and 260 nm of thickness presented a friction coefficient of ~0.73 equal to that obtained for the uncoated XC100 steel substrate.

The films deposited during 90 min showed friction coefficient values around 0.65 (10%N_2) and 0.60 (20%N_2). A significant improvement was observed with increasing the deposition time (film thickness) and the lowest values were obtained for the thickest film deposited during 180 min (μ = ~0.43). This low-friction effect was explained by previous studies where the dense structure and the formation of vanadium oxide layer, including V_2O_5, serve as a lubricant between two counterparts in contact [6,36]. However, the high values of friction coefficients of the V−N thinner films deposited for short period (20–60 min, film thicknesses are less than 1 μm) could be due to their high roughness (Table 1).

In a thin film, the plastic deformation zone at the film/substrate interface is important, which probably influences the friction behavior and increases the standard deviation. On the other hand, after few meters of sliding distance, the friction coefficient achieved its maximum value of 0.78. According to Kumar et al. [3], the contact stress may be lower than that of the material intrinsic stress at the film/steel substrate interface during the initial sliding tests. In the literature, we found that the origin of low friction and high wear resistance behavior of Ti−N films are directly correlated to the change in preferred crystalline orientation. It has been reported that (111) crystalline plane has low friction due to higher packing density [3].

In contrast, the maximum values were reached and stabilized after few sliding cycles for the thicker films with very narrow wear tracks. This is due to the contact stress, which does not affect the film/substrate interface. Wear tests showed that the V−N coatings deposited under 10%N_2 have a higher friction coefficient compared to the other coatings deposited under 20%N_2. The presence of V_2O_5 in superficial zone of the V−N coatings deposited under 20%N_2 plays the role of a lubricant and led to decrease the friction coefficient [1,41]. In a similar study on the Cr-N/V-N films, Yuexiu et al. [41] explained the low friction coefficient of these films by the presence of vanadium oxides. In the case of V−N coating, the presence of oxides within the film may play an important role in the reduction of friction coefficient.

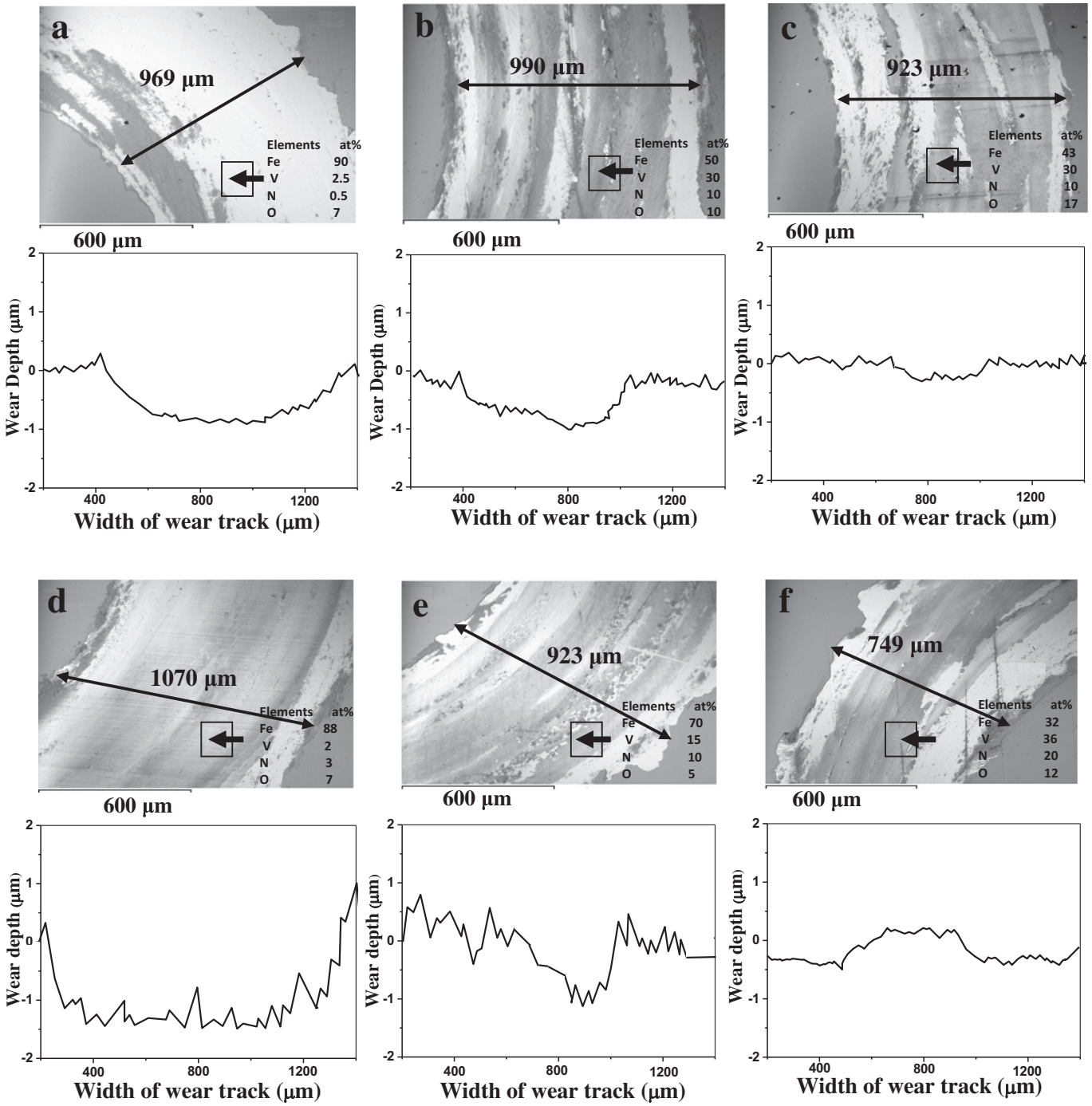

Fig. 10. SEM images, depth and width of wear tracks of V−N films deposited at 20%N_2: a) 260 nm, b) 960 nm and c) 1800 nm and at 10%N_2: d) 300 nm, e) 1200 nm and f) 2500 nm of thickness.

3.5.2. Wear resistance

The SEM images, width and depth profiles of the wear tracks made on the V−N films by a100Cr6 ball in dry conditions are illustrated in Fig. 10. Increasing the nitrogen content in the V−N films, by increasing its percentage from 10 to 20% in the deposition gas mixture atmosphere, improved the wear resistance. Since the nitrogen is well known as a lubricating, the incorporation of more nitrogen into vanadium could lubricate the wear track and reduce the interaction between the film and the 100Cr6 counterpart leading to a gradual decrease in friction coefficient.

However, the films deposited under 10%N_2 presented relatively high wear rate and track depth compared to the other films deposited under 20%N_2. This may be due to the large amount of hexagonal V_2N phase that plays the role of an abrasive body causing severe wear. In addition, the increase of surface roughness when nitrogen content in a V−N film decreases, can be explain the increase of its wear track [42]. From Fig. 11, the wear tracks of the V−N films deposited, under 10 and 20%N_2, for 20 min were large (1070, 969 µm), deep (1.26, 1.06 µm) and their wear rates were 11.6 and 7.6 ($\times 10^{-6}$ m^3/N·m), respectively. The grooves found in the wear track were due to the detachment of the films. This is because of the low resistance of films to plastic deformation characterizing the abrasive wear. The EDS analysis showed that there was no a significant quantity of coating elements at the adhesive wear tracks of V-N/XC100. The Fe of substrate and O were

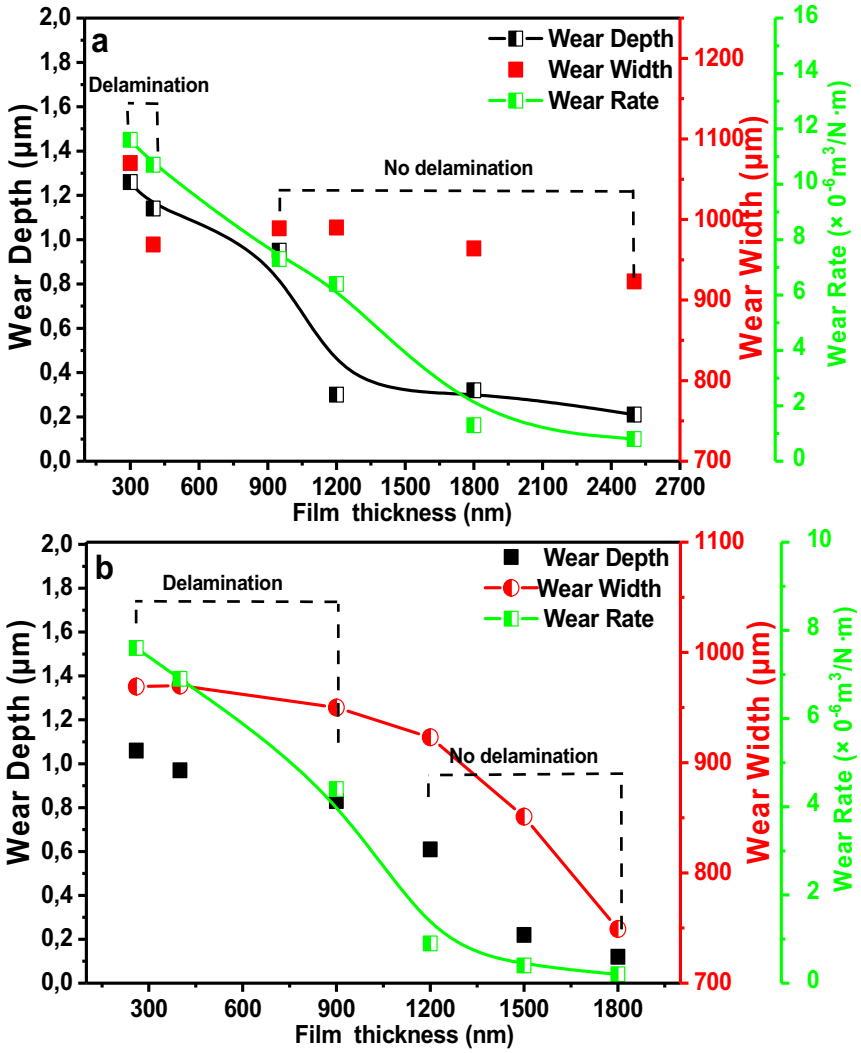

Fig. 11. Wear rate, depth and width of V–N films deposited at a) 10%N_2 and b) 20% N_2 for different film thicknesses.

clearly detected in the wear tracks.

The SEM images show that the wear depth was gradually decreased with increasing the film thickness for both series of V–N films (deposited under 10 and 20%N_2). For the thinner V–N films, the contact area was large (Fig. 10a–d) and a total delamination was occurred in the films. According to Ali et al. [43], the contact stress is prominent, which would increase the plastic deformation and wear takes place during the initial sliding passes and the shear resistance of the film becomes weaker as a result of the high contact pressure between the film and the ball counterpart. However, increasing the film thickness of the V–N film resulted in the decrease in depth, width and rate of the wear track showing an improvement in wear resistance of the film (Figs. 10 and 11). The V–N films deposited during 90 min (Fig. 10b–e) showed the narrowest widths and shallowest depths. In fact, the contact stress without affecting the film/substrate interface results in a higher shear resistance with negligible grooves, especially for the films deposited under 20%N_2 (Fig. 11). This may be due to the increase in the concentrations of V (30 at.%) and N (10 at.%) and the decrease in the concentration of Fe (43 at.%) in the analyzed wear track for the films deposited under 20%N_2 (Fig. 10c). The dense structure and the smooth surface of the thick films contributed to the improvement of their wear resistance and to reduce their friction coefficient. In addition, the high H^3/E^2 values and the enhancement of film hardness lead to increase its resistance against plastic deformation and wear [22].

4. Conclusion

In this paper, we studied the vanadium nitride thin films deposited by magnetron sputtering. We focused on the influence of film thickness and nitrogen percentage in the gas deposition atmosphere on their structure, mechanical and tribological properties. The XRD analysis revealed the polycrystalline structure of the V–N films. It has been found that the nitrogen ratio in the N_2/Ar mixture atmosphere influenced the film crystallinity. In the V–N films deposited under 10%N_2, the (200) VN plane was observed, whereas, (111) VN plane was predominant under 20%N_2 with a mixture of (hc) V_2N and (fcc) VN phases.

Furthermore, we obtained the following results:

- With increasing the film thickness, the crystallite refinement was proven to enhance the coating mechanical properties and therefore the adhesion strength by increasing the resistance to plastic deformation (H^3/E^2).
- The variation of mechanical properties was associated to the microstructural features depending on the film thickness.
- The dense structure, smooth surface and (111) VN predominant plane for the thicker film led to enhance the film hardness, deposited under 20%N_2, and consequently improved its tribological properties.
- The decrease of V–N film friction with increasing its thickness was due to its strong adhesion leading to enhance its tribological

behavior in a dry environment.

- The reduction of wear rate in the thicker films was explained by the improvement in crystallinity and microstructural properties.

Acknowledgements

The authors would like to thank Pr. Luc IMHOFF for the SEM and XPS analysis of the test samples at LICB-University of Burgundy in Dijon. The authors are also grateful to the laboratories' teams: MSMP at ENSAM-Lille and LaBoMaP at Arts et Metiers Paris Tech of Cluny for their help in the deposition and characterization of coatings.

References

[1] Y. Qiu, S. Zhang, B. Li, Y. Wang, J.-W. Lee, F. Li, D. Zhao, Improvement of tribological performance of CrN coating via multilayering with VN, Surf. Coat. Technol. 231 (2013) 357–363.
[2] J.C. Caicedo, W. Aperador, C. Amaya, Determination of physical characteristic in vanadium carbon nitride coatings on machining tools, Int. J. Adv. Manuf. Technol. 91 (1–4) (2017) 1227–1241.
[3] D.D. Kumar, N. Kumar, S. Kalaiselvam, R. Thangappan, R. Jayavel, Film thickness effect and substrate dependent tribo-mechanical characteristics of titanium nitride films, Surfaces Interfaces 2468-0230 (2018) (30246-3).
[4] H.S. Akkera, N.N. Reddy, M.C. Sekhara, Thickness dependent structural and electrical properties of magnetron sputtered nanostructured CrN thin films, Mater. Res. 20 (3) (2017) 712–717.
[5] L. Aissani, M. Fellah, C. Nouveau, M.A. Samad, A. Montagne, A. Iost, Structural and mechanical properties of Cr–Zr–N coatings with different Zr content, Surf. Eng. 35 (2017) 1–9.
[6] L. Aissani, C. Nouveau, M.J. Walock, H. Djebaili, A. Djelloul, Influence of vanadium on structure, mechanical and tribological properties of CrN coatings, Surf. Eng. 31 (10) (2015) 779–788.
[7] H. Guo, C. Lu, Z. Zhang, B. Liang, J. Jia, Comparison of microstructures and properties of VN and VN/Ag nanocomposite films fabricated by pulsed laser deposition, Appl. Phys. A Mater. Sci. Process. 124 (2018) 694–701.
[8] A.M. Glushenkov, D.H. Jurcakova, D. Llewellyn, G. Lu, Y. Chen, Structure and capacitive properties of porous nanocrystalline VN prepared by temperature-programmed ammonia reduction of V_2O_5, Chem. Mater. 22 (2010) 914–921.
[9] M.A. Roldan, V.L. Flores, M.D. Alcala, A. Ortega, C. Real, Mechanochemical synthesis of vanadium nitride, J. Eur. Ceram. Soc. 30 (2010) 2099–2107.
[10] J.C. Caicedo, G. Zambrano, W. Aperador, L. Escobar-Alarcon, E. Camps, Mechanical and electrochemical characterization of vanadium nitride (VN) thin films, Appl. Surf. Sci. 258 (2011) 312–320.
[11] J. Huotari, R. Bjorklund, J. Lappalainen, A. Lloyd Spetz, Pulsed laser deposited nanostructured vanadium oxide thin films characterized as ammonia sensors, Sensors Actuators B Chem. 217 (2015) 22–29.
[12] X.H. Zheng, D.G. Walmsley, Discrepancy between theory and measurement of superconducting vanadium, Physica C 515 (2015) 41–48.
[13] I. Galesic, U. Reusch, C. Angelkort, H. Lewalter, A. Berendes, E. Schweda, Nitridation of vanadium in molecular nitrogen: a comparison of rapid thermal processing (RTP) and conventional furnace annealing, Vacuum 61 (2003) 479–484.
[14] I. Mayrhuber, C.R. Dennison, V. Kalra, E.C. Kumbur, Laser-perforated carbon paper electrodes for improved mass-transport in high power density vanadium redox flow batteries, J. Power Sources 260 (2014) 251–258.
[15] S.-Y. Chun, Properties of VN coatings deposited by ICP assisted sputtering: effect of ICP power, J. Korean Ceram. Soc. 54 (1) (2017) 38–42.
[16] F. Ge, P. Zhu, F. Meng, Q. Xue, F. Huang, Achieving very low wear rates in binary transition-metal nitrides: the case of magnetron sputtered dense and highly oriented VN coatings, Surf. Coat. Technol. 248 (15) (2014) 81–90.
[17] B. Krause, M. Kaufholz, S. Kotapati, R. Schneider, E. Müller, D. Gerthsen, P. Wochner, T. Baumbach, Angle-resolved X-ray reflectivity measurements during off-normal sputter deposition of VN, Surf. Coat. Technol. 277 (C) (2015) 52–57.
[18] L. Aissani, A. Alhussein, C. Nouveau, L. Radjehi, I. Lakdhar, E. Zgheib, Evolution of microstructure, mechanical and tribological properties of vanadium carbonitride coatings sputtered at different nitrogen partial pressures, Surf. Coat. Technol. 374 (2019) 531–540.
[19] Y. Qiu, S. Zhang, B. Li, J.-W. Lee, D. Zhao, Influence of nitrogen partial pressure and substrate bias on the mechanical properties of VN coatings, Procedia Eng. 36 (2012) 217–225.
[20] H. Guo, B. Li, J. Wang, W. Chen, Z. Zhang, W. Wang, J. Jia, Microstructures, mechanical and tribological properties of VN films deposited by PLD technique, RSC Adv. 6 (40) (2016) 1–16.
[21] H. Gueddaoui, S. Maabed, G. Schmerber, M. Guemmaz, J.C. Parlebas, Structural and optical properties of vanadium and hafnium nitride nanoscale films: effect of stoichiometry, Eur. Phys. J. B 60 (2007) 305–312.
[22] H. Ju, D. Yu, J. Xu, L. Yu, Y. Geng, T. Gao, G. Yi, S. Bian, Microstructure, mechanical, and tribological properties of niobium vanadium carbon nitride films, J. Vac. Sci. Technol. A 36 (3) (2018) 1–7.
[23] H. Zhao, L. Yu, C. Mu, F. Ye, Structure and properties of Si-implanted VN coatings prepared by RF magnetron sputtering, Mater. Charact. 117 (2016) 65–75.
[24] B. Tlili, C. Nouveau, M.J. Walock, M. Nasri, T. Gharib, Effect of layer thickness on thermal properties of multilayer thin films produced by PVD, Vacuum 86 (8) (2016) 1048–1056.
[25] T. Elangovan, P. Kuppusami, R. Thirumurugesan, V. Ganesan, E. Mohandas, D. Mangalaraj, Nanostructured CrN thin films prepared by reactive pulsed DC magnetron sputtering, Mater. Sci. Eng. B 167 (2010) 17–25.
[26] Y. Zhang, X.-H. Yan, W.-B. Liao, K. Zhao, Effects of nitrogen content on the structure and mechanical properties of (Al0.5CrFeNiTi0.25)Nx high-entropy films by reactive sputtering, Entropy 20-624 (2018) 1–12.
[27] S. Mahieu, P. Ghekiere, D. Depla, R. De Gryse, Biaxial alignment in sputter deposited thin films, Thin Solid Films 515 (2006) 1229–1249.
[28] L. Aissani, M. Fellah, L. Radjehi, C. Nouveau, A. Montagne, A. Alhussein, Effect of annealing treatment on the microstructure, mechanical and tribological properties of chromium carbonitride coatings, Surf. Coat. Technol. 359 (2019) 403–413.
[29] H.-N. Shah, Structural and mechanical characterization of the chromium nitride hard coating deposited on the silicon and glass substrate, Int. J. Automotive Mech. Eng. 14 (1) (2017) 3872–3886.
[30] X. Chu, S.A. Barnett, M.S. Wong, W.D. Sproul, Reactive magnetron sputters deposition of polycrystalline vanadium nitride films, J. Vac. Sci. Technol. A 14 (6) (1996) 3124–3129.
[31] N. Ouldhamadouche, A. Achour, R. Lucio-Porto, M. Islam, S. Solaymani, A. Arman, A. Ahmadpourian, H. Achour, L. Brizoual, M.A. Djouadi, T. Brousse, Electrodes based on nano-tree-like vanadium nitride and carbon nanotubes for micro-supercapacitors, J. Mater. Sci. Technol. 34 (2018) 976–982.
[32] C.M. Ghimbeu, E. Raymundo-Pinero, P. Fioux, C. Vix-Guterl, Vanadium nitride/carbon nanotube nanocomposites as electrodes for supercapacitors, J. Mater. Chem. 21 (2011) 13268–13275.
[33] L. Wang, J. Teng, P. Liu, A. Hirata, E. Ma, Z. Zhang, M. Chen, X. Han, Grain rotation mediated by grain boundary dislocations in nanocrystalline platinum, Nat. Commun. 5 (2014) 1–7.
[34] O. Bondarchuk, A. Morel, D. Belanger, E. Goikolea, T. Brousse, R. Mysyk, Thin films of pure vanadium nitride: evidence for anomalous non-faradaic capacitance, J. Power Sources 324 (2016) 439–446.
[35] D. Gall, R.T. Haasch, N. Finnegan, T.-Y. Lee, C.-S. Shin, E. Sammann, J.E. Greene, I. Petrov, In situ X-ray photoelectron, ultraviolet photoelectron, and auger electron spectroscopy spectra from first-row transition-metal nitrides: ScN, TiN, VN and CrN, Surf. Sci. Spectra 7 (3) (2000) 167–168.
[36] A. Glaser, S. Surnev, F.P. Netzer, N. Fateh, G.A. Fontalvo, C. Mitterer, Oxidation of vanadium nitride and titanium nitride coatings, Surf. Sci. 601 (2007) 1153–1159.
[37] G. Gassner, P.H. Mayrhofer, K. Kutschej, C. Mitterer, M. Kathrein, A new low friction concept for high temperatures: lubricious oxide formation on sputtered VN coatings, Tribol. Lett. 17 (4) (2004) 751–756.
[38] J.-H. Huang, H.-C. Yang, X.-J. Guo, G.-P. Yu, Effect of film thickness on the structure and properties of nanocrystalline ZrN thin films produced by ion plating, Surf. Coat. Technol. 195 (2005) 204–213.
[39] S. Veprek, G.J.V.-H. Maritza, P. Karvankova, J. Prochazka, Different approaches to superhard coatings and nanocomposites, Thin Solid Films 4765 (1) (2005) 1–29.
[40] W.-J. Chou, G.-P. Yu, J.-H. Huang, Deposition of TiN thin films on Si (100) by HCD ion plating, Surf. Coat. Technol. 140 (3) (2001) 206–214.
[41] Q. Yuexiu, S. Zhang, B. Li, Y. Wang, J.-W. Lee, F. Li, D. Zhao, Improvement of tribological performance of CrN coating via multilayering with VN, Surf. Coat. Technol. 231 (2013) 126–130.
[42] I. Bouabibsa, S. Lamri, A. Alhussein, T. Minea, F. Sanchette, Plasma investigations and deposition of metal doped Me-DLC (Me = Al, Ti or Nb) obtained by a magnetron sputtering-RFPECVD hybrid process, Surf. Coat. Technol. 354 (2018) 351–359.
[43] R. Ali, M. Sebastiani, E. Bemporad, Influence of Ti–TiN multilayer PVD-coatings design on residual stresses and adhesion, Mater. Des. 75 (2015) 47–56.